Molecular Neurobiology (2019) 56:5844–5855
https://doi.org/10.1007/s12035-019-1485-6

Impaired Pentose Phosphate Pathway in the Spinal Cord of the hSOD1^{G93A} Mouse Model of Amyotrophic Lateral Sclerosis

Tesfaye Wolde Tefera[1,2] · Katherine Bartlett[1] · Shirley S. Tran[1] · Mark P. Hodson[3,4,5] · Karin Borges[1]

Received: 6 November 2018 / Accepted: 10 January 2019 / Published online: 26 January 2019

Abstract

Impairments in energy metabolism in amyotrophic lateral sclerosis (ALS) have long been known. However, the changes in the energy-producing pathways in ALS are not comprehensively understood. To investigate specific alterations in glucose metabolism in glycolytic, pentose phosphate, and TCA cycle pathways, we injected uniformly labeled [U-^{13}C]glucose to wild-type and hSOD1^{G93A} mice at symptom onset (80 days). Using liquid chromatography-tandem mass spectrometry (LC-MS/MS), levels of metabolites were determined in extracts of the cortex and spinal cord. In addition, the activities of several enzymes involved in glucose metabolism were quantified. In the spinal cord, the levels of pentose phosphate pathway (PPP) intermediate ribose 5-phosphate ($p = 0.037$) were reduced by 37% in hSOD1^{G93A} mice, while the % ^{13}C enrichments in glucose 6-phosphate were increased threefold. The maximal activities of the enzyme glucose 6-phosphate dehydrogenase were decreased by 24% in the spinal cord ($p = 0.005$), suggesting perturbations in the PPP. The total amount of pyruvate in the cortex ($p = 0.039$) was reduced by 20% in hSOD1^{G93A} mice. Also, the activities of the glycolytic enzyme pyruvate kinase were reduced in the cortex by 31% ($p = 0.002$), indicating alterations in glycolysis. No significant differences were seen in the total amounts as well as % ^{13}C enrichments in most TCA cycle intermediates, suggesting largely normal TCA cycle function. On the other hand, oxoglutarate dehydrogenase activity was decreased in the cortex, which may indicate increased oxidative stress. Overall, this study revealed decreased activity of the PPP in the spinal cord and alterations in glycolysis in hSOD1^{G93A} mouse CNS tissues at the early symptomatic stage of disease.

Keywords Energy metabolism · Glycolysis · Liquid chromatography-tandem mass spectrometry · Motor neuron disease · Pentose phosphate pathway · TCA cycle

Introduction

Amyotrophic lateral sclerosis (ALS) is a progressive neurodegenerative disease that causes selective death of neurons in the cortex and the spinal cord [1]. Most cases (90%) of ALS are sporadic, while about 10% are familial. Mutations in the superoxide dismutase 1 (SOD1) gene constitutes 20% of familial ALS cases, and the hSOD1^{G93A} mouse model is the most widely characterized model of ALS [2]. The exact mechanisms of motor neuron death in this disease are not comprehensively known. Several mechanisms have been hypothesized, including abnormal protein aggregation [3], glutamate excitotoxicity [4, 5], oxidative stress [6], and dysfunctional energy metabolism [7, 8]. It is likely that a combination of these pathogenic mechanisms contributes to the pathogenesis and progression of ALS.

Alterations in energy metabolism in people with ALS as well as ALS animal models have been reported in various studies. Many patients with ALS display abnormal energy

Electronic supplementary material The online version of this article (https://doi.org/10.1007/s12035-019-1485-6) contains supplementary material, which is available to authorized users.

✉ Karin Borges
k.borges@uq.edu.au

[1] Neurological Disorders and Metabolism Lab, School of Biomedical Sciences, The University of Queensland, Brisbane, QLD 4072, Australia

[2] Present address: Australian Institute for Bioengineering and Nanotechnology, The University of Queensland, Brisbane, Australia

[3] Metabolomics Australia Queensland Node, Australian Institute for Bioengineering and Nanotechnology, The University of Queensland, Brisbane, Australia

[4] School of Pharmacy, The University of Queensland, Brisbane, Australia

[5] Present address: Metabolomics Research Laboratory, Victor Chang Cardiac Research Institute, Sydney, Australia

homeostasis and reduced body weight, indicating defects in whole-body energy metabolism [9, 10]. In certain CNS regions, including the cortex and spinal cord, several fluorodeoxyglucose positron emission tomography (FDG-PET) and ^{14}C autoradiography studies have indicated glucose hypometabolism in patients and in animal models of ALS [11–13]. Consistent with this, we demonstrated that glycolysis-derived metabolites and first-turn TCA cycle–derived metabolites were significantly reduced in the cortex and spinal cord of the hSOD1^{G93A} mouse model of ALS at symptomatic stages of the disease, indicating reduced glycolysis [14]. Specifically, we measured the levels of metabolites of injected [1-^{13}C]glucose and [1,2-^{13}C]acetate using high-pressure liquid chromatography (HPLC) and ^{1}H and ^{13}C nuclear magnetic resonance spectroscopy (NMR spectroscopy). We found reduced total lactate, [3-^{13}C]lactate, total alanine, and [3-^{13}C]alanine concentrations mainly in the CNS at mid stage, while the levels of glucose were largely unaltered [14].

There is little known about alterations in defined glycolytic and TCA cycle steps, nor the activity of the pentose phosphate pathway (PPP) in ALS. The PPP is strongly connected to glycolysis and is important for the generation of NADPH, which may protect cells from oxidative stress. Although increased oxidative damage has been reported in CNS tissues of patients with ALS and animal models (reviewed in [15, 16]), there are few studies about alterations of the PPP in ALS thus far.

Several impairments in the TCA cycle pathway have been reported in ALS models [17]. Reduced gene expression of the TCA cycle enzymes isocitrate dehydrogenase and oxoglutarate dehydrogenase was found in the CNS tissues from hSOD1^{G93A} mice [18, 19], which could lead to diminished metabolism of glucose via the TCA cycle. In our previous study, we found reduced labeling of first-turn TCA cycle–derived metabolites from [1-^{13}C]glucose, including [4-^{13}C]glutamate, [4-^{13}C]glutamine, and [2-^{13}C] GABA, which indicates reduced entry of [3-^{13}C]pyruvate into the TCA cycle and reduced availability of TCA cycle intermediates for amino acid and neurotransmitter generation [14].

Collectively, abnormalities in the energy-producing pathways in ALS may lead to reduced ATP generation and subsequent death of neurons (reviewed in [20, 21]). However, the specific pathologic changes in each of these pathways contributing to the generation of reduction equivalents, energy, riboses, neurotransmitters, amino acids, and lipids are not clearly understood. The aim of this study was to further investigate alterations in glycolysis, the pentose phosphate, and TCA cycle pathways in the brain and spinal cord tissues from hSOD1^{G93A} mice at symptomatic stage of the disease. Thus, we examined the activity of glycolysis, pentose phosphate, and TCA cycle pathways in vivo in the brain and spinal cord of wild-type and hSOD1^{G93A} mice at onset of disease (80 days). We studied the metabolism of uniformly labeled glucose ([U-^{13}C])glucose in vivo quantifying metabolites by liquid chromatography-tandem mass spectrometry (LC-MS/MS) and investigated the activities of enzymes involved in glucose metabolism in tissue extracts.

Methods

Animals

All animal experiments were approved by the University of Queensland Animal Ethics Committee (SBMS 128/14) and followed the guidelines of the Queensland Animal Care and Protection Act 2001. Wild-type and hSOD1^{G93A} mice were bred by mating hSOD1^{G93A} males expressing high copy number of mutant SOD1 (B6.Cg-Tg(SOD1*G93A)1Gur/J, Jackson laboratory, Bar Harbor, ME, USA) with C57BL/6 wild-type females (University of Queensland). Female mice at 80 days (onset of disease) were used for this experiment. Mice were maintained in a 12-h light, 12-h dark cycle and had access to food and water ad libitum. Animals were randomly assigned numbers for tissue extraction as well as LC-MS/MS, enzyme activity, and data analyses. The genotype of the two groups was revealed after all the analysis was completed. All efforts were made to reduce the numbers and suffering of animals.

Injection of Uniformly Labeled Glucose ([U-^{13}C] Glucose)

Wild-type ($n = 13$) and hSOD1^{G93A} mice ($n = 14$) at 80 days (onset of disease) were injected with uniformly labeled glucose ([U-^{13}C]glucose, 0.3 M i.p., Cambridge Isotope Laboratories, Tewksbury, MA, USA). After 15 min, mice were killed by microwave fixation to the head (Model MMW-05, Muromachi, Tokyo, Japan) at 5 KW for 0.74 to 0.80 s, to denature enzymes quickly. The cortex and the lumbar sections of the spinal cord tissues were dissected and stored at − 80 °C until extracted. The spinal cord tissues were not microwave-fixated and therefore subject to post-mortem metabolism. The time taken to dissect and freeze the spinal cord was less than 60 s.

Extraction of Tissue

The cortical and spinal cord tissues were first homogenized with a sonicator (Branson ultrasonics, Danbury, CT, USA) with an initial solvent of 1000 μl for the cortex and 750 μl for the spinal cord samples of chilled methanol with the addition of 4 μl or 3 μl of 1 mM azidothymidine (AZT) as an internal standard, respectively. Water-soluble metabolites were extracted using methanol/water/chloroform extraction method as described in [22]. Samples were dried and metabolites quantified by liquid chromatography-tandem mass spectrometry (LC-MS/MS).

Labeling Patterns of [U-^{13}C]Glucose

Via glycolysis, [$^{13}C_6$]glucose is phosphorylated into [U-^{13}C]glucose-6-phosphate (G6P) by hexokinase. G6P gets further metabolized into uniformly labeled ([U-^{13}C])fructose-6-phosphate (F6P), fructose-1,6 diphosphate (F16DP), dihydroxyacetone phosphate (DHAP), glyceraldehyde 3-phosphate (GA3P), 1,3 bisphosphoglycerate (13BPG, not measured), (2 + 3) phosphoglycerate (2 + 3 PG), phosphoenol pyruvate (PEP), and pyruvate (PYR) and lactate (LAC). [U-^{13}C]G6P can also be metabolized to glucose 1-phosphate (G1P) or enter the pentose phosphate pathway to produce uniformly labeled ribose 5-phosphate (R5P), ribulose 5-phosphate (RL5P) and xylulose 5-phosphate (X5P). Metabolites of the PPP can re-enter glycolysis as glyceraldehyde 3-phosphate (GA3P). [U-^{13}C]pyruvate enters into the TCA cycle as [1, 2-^{13}C]acetyl CoA via pyruvate dehydrogenase (PDH). In the first turn of the TCA cycle, if [1, 2]acetyl CoA condenses with unlabeled oxaloacetate (OAA), it forms M + 2–labeled citrate (CIT), aconitate (ACO), α-ketoglutarate (AKG), succinate (SUC), fumarate (FUM), malate (MAL), and OAA (see Fig. 1). In the second turn of the TCA cycle, [1, 2]acetyl CoA condenses with labeled (M + 2) oxaloacetate (OAA) to give rise to (M + 4) labeled CIT and AKG, (M + 3) SUC, FUM, and MAL. For detailed labeling pattern and mass isotopomer analysis, see [23].

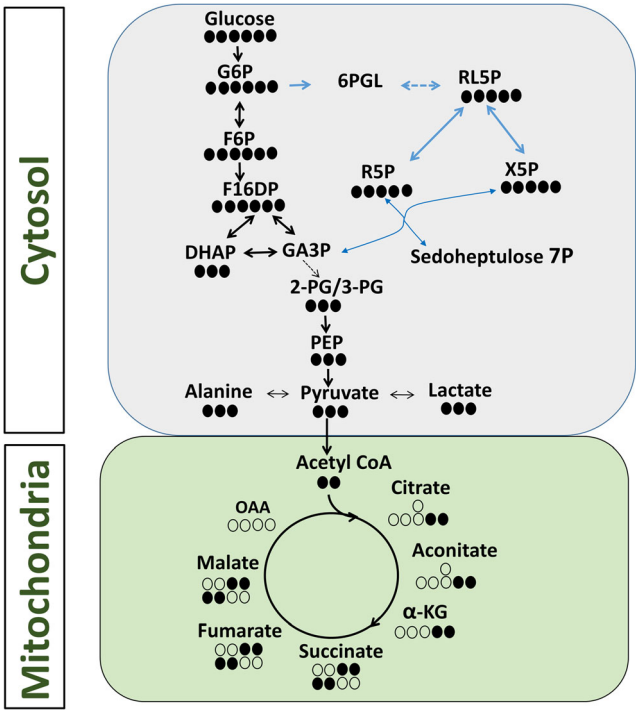

Fig. 1 Labeling patterns of selected glycolytic, pentose phosphate, and first-turn TCA cycle intermediates following metabolism of [U-^{13}C]glucose. ^{13}C-labeled carbons are shown as black circles while unlabeled carbons are represented as white circles. G6P, glucose 6-phosphate; 6PGL, 6-phospho gluconolactone; F6P, fructose 6-phosphate; F16DP, fructose 1,6-bisphosphate; DHAP, dihydroxyacetone phosphate; GA3P, glyceraldehyde 3-phosphate; (2/3) PG, 2 + 3 phosphoglycerate; PEP, phosphoenol pyruvate; RL5P, ribulose 5-phosphate; R5P, ribose 5-phosphate; X5P, xylulose 5-phosphate; OAA, oxaloacetate; α-KG, α-ketoglutarate

Liquid Chromatography-Tandem Mass Spectrometry

LC-MS/MS data were obtained as described in [23, 24]. Total amounts of metabolites were corrected using the weight of extracted tissue and internal standard added. For % ^{13}C enrichment analysis, 1.1% natural abundant ^{13}C was subtracted. Two wild-type and three hSOD1^{G93A} samples without ^{13}C labeling, which were likely a result of misdirected injection of labeled glucose, were removed from the analysis.

Enzyme Assays

The maximal activities of cytosolic (hexokinase (HK), pyruvate kinase (PK), glucose 6-phosphate dehydrogenase (G6PDH) and pyruvate dehydrogenase (PDH)), and mitochondrial enzymes (oxoglutarate dehydrogenase (OGDH), glutamic oxaloacetic transaminase (GOT), glutamate dehydrogenase (GDH)) involved in energy metabolism were quantified in extracts of wild-type and hSOD1^{G93A} mice cortex and the spinal cord as previously described in [23, 25]. All enzyme assays were performed with the investigators blinded to the genotype of the samples.

Cytosolic and Mitochondrial Enrichment

Wild-type ($n = 11$) and hSOD1^{G93A} mice ($n = 15$) were sacrificed at disease onset (80 days of age). Brains and spinal cortices were removed, snap-frozen in dry ice, and stored at − 80 °C until required. The cortex and the spinal cord tissues were homogenized in 500 μL of mitochondrial enrichment buffer (70 mM sucrose, 210 mM mannitol, 5 mM HEPES; pH 7.4) with the addition of 5 μL of protease inhibitor cocktail (cat no. P8340, Sigma-Aldrich, NSW, Australia) using a glass-Teflon homogenizer. Samples were centrifuged at 1000*g*, 4 °C for 10 min, and the supernatant was transferred to a new tube and centrifuged again at 12,000*g*. The supernatant (cytosolic fraction) was removed and the pellet was resuspended in 250 μL mitochondrial isolation buffer (with added 1 mM EDTA and 0.5% BSA) and centrifuged at 10,500*g*. The pellet was resuspended in 150 μL mitochondrial isolation buffer (mitochondrial enriched fraction). Both fractions were aliquoted and stored at − 80 °C.

Continuous Spectrophotometric Assays

The activities of HK, PK, G6PDH, GDH, and GOT were determined through continuous spectrophotometric assays using the Spectramax 190 Microplate Reader (Molecular Devices,

CA, USA) as previously described in [23]. A Pierce bicinchoninic acid (BCA) assay (Thermo Fisher Scientific) was performed to determine protein concentration in each sample. The activities of GDH, GOT, and PK were determined via the oxidation of reduced β-nicotinamide adenine dinucleotide (β-NADH), while the activities of HK and G6PDH were measured through the reduction of β-nicotinamide adenine dinucleotide phosphate (β-NADP+) at 340 nm. In a 96-well plate, 10–30 μg of each sample was added to a reaction mix. To measure GDH activity, 25 mM 2-oxoglutarate (2-OG) (initiating reagent) was added to a reaction mix consisting of 100 mM potassium phosphate (pH 7.4), 0.6 mM β-NADH, and 105 mM ammonium chloride. For GOT, 3 mM aspartate was added to 80 mM Tris-HCl (pH 7.8), 0.6 mM β-NADH, 15 mM 2-OG, and 8.5 U/mL malic dehydrogenase (cat. M1567, Sigma-Aldrich, NSW, Australia). For PK, 20 mM phosphoenol pyruvate was added to 70 mM imidazole buffer (pH 7.2), 5 mM ADP, 40 mM $MgCl_2$, 50 mM KCl, 0.6 mM β-NADH, and 24 U/mL lactic dehydrogenase (cat. L2500, Sigma-Aldrich, NSW, Australia). For HK, 200 mM D-glucose was added to 200 mM triethanolamine buffer (pH 7.4), 60 mM ATP, 20 mM β-NADP, 600 mM MgCl2, and 0.4 U G6PDH. For the G6PDH assay, 15 mM G6P was added to 85 mM Tris-HCl (pH 7.4), 2 mM β-NADP, and 100 mM $MgCl_2$. The initiating reagents were added just prior to the measurement of enzyme activity. The linear portion of the change in absorbance was measured, and the enzyme activity was calculated using the following equation.

$$\text{Activity}(\text{nmol}/\text{min}/\text{mL}) = \frac{\Delta\, Abs/\text{min} \times \text{dilution factor} \times \text{total volume of assay (mL)} \times 1000}{\text{mM extinction coefficient} \times \text{volume of enzyme (mL)}}$$

The tests were performed in triplicate, and the activity was expressed as nmol/min/mL, normalized to protein content (determined from the BCA assay), and finally expressed as U/mg protein.

Continuous Fluorometric Assays

The activities of PDH and OGDH were determined using the Spectramax M4 Multi-Mode Microplate Reader (Molecular Devices, CA, USA) through continuous fluorometric assays as previously described by [25]. The same procedure was followed except 60 μg of the sample (mitochondrial fraction) was used and the reduction of β-NAD+ was measured at 355-nm excitation and 460-nm emission. For PDH, 2 mM sodium pyruvate was added to 35 mM potassium phosphate (pH 7.4), 1 mM $MgCl_2$, 0.175 mM thiamine pyrophosphate, 2 mM β-NAD, 2.5 mM dithiothreitol, 0.15 mM coenzyme A, and 0.04 mM rotenone. For OGDH, 1 mM 2-OG was added to 50 mM HEPES (pH 7.4), 1 mM $MgCl_2$, 1 mM coenzyme A, 0.2 mM thiamine pyrophosphate, 4 mM β-NAD, 0.5 mM dithiothreitol, and 0.04 mM rotenone. Enzyme activities were expressed as units of relative fluorescence/min/mg protein and normalized to activities found in tissues from wild-type mice.

Data Analysis

The comparisons of metabolite levels and activities of cytosolic and mitochondrial enzymes in the cortex and spinal cord between wild-type and $hSOD1^{G93A}$ mice were performed using Student's unpaired t test. $p < 0.05$ was regarded to be significant. Data were analyzed using GraphPad Prism 7 (GraphPad, San Diego, USA) and are expressed as mean ± SEM.

Results

The total amounts as well as % ^{13}C enrichments (the amount of label corrected for natural abundance ^{13}C over the total amount of metabolite) of glycolytic, PPP, and TCA cycle metabolites from extracts of the cortex and spinal cord of wild-type and $hSOD1^{G93A}$ mice injected with [U-^{13}C]glucose at onset of disease (80 days) were determined using LC-MS/MS. Also, the maximal activities of enzymes involved in glucose metabolism were investigated in extracts from wild-type and $hSOD1^{G93A}$ mouse brains and spinal cords.

Total Amounts and % ^{13}C Enrichments of Glycolytic and PPP Intermediates

The total amounts of the glycolytic metabolite pyruvate (PYR) were significantly reduced by 20% in the cortex of $hSOD1^{G93A}$ mice compared with wild-type mice (Fig. 2a, $p = 0.039$). There were no significant differences in the total amounts of G6P, F6P, F16DP, DHAP, 2 + 3 PG, R5P and PEP in the cortex (Fig. 2a). In the spinal cord, the total amounts of the PPP metabolite R5P ($p = 0.037$) were significantly diminished by 35% (Fig. 2b). No significant differences were seen in the total amounts of G6P, F6P, F16DP, DHAP, (2 + 3) PG, PEP, and PYR (Fig. 2b). We found increased % ^{13}C enrichments by 26% in F16DP (M + 6) in the cortex ($p = 0.038$) and threefold in G6P (M + 6) in the spinal cord ($p = 0.04$) of $hSOD1^{G93A}$ mice, while there were no significant changes

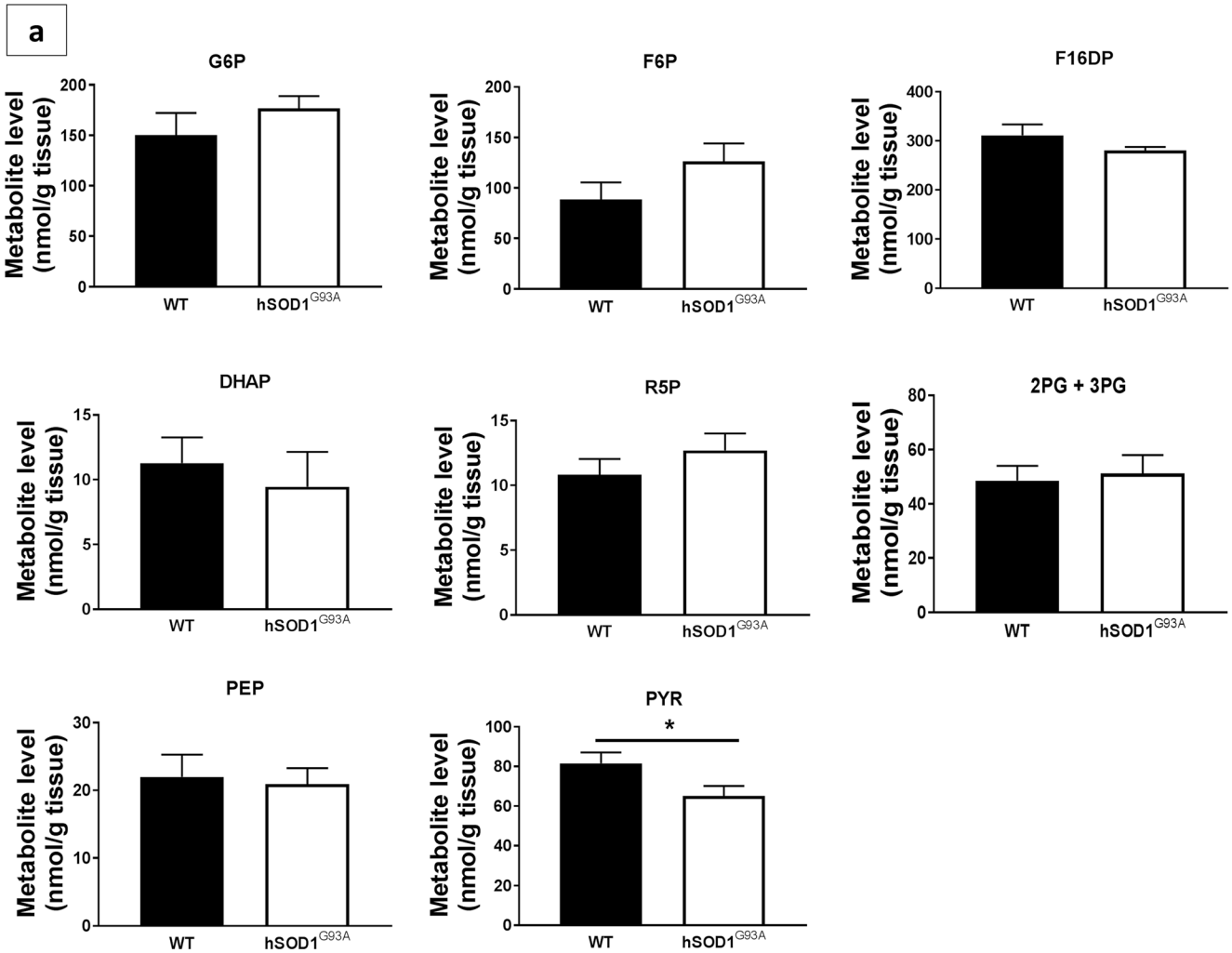

Fig. 2 Total amounts (nmol/g tissue) of selected glycolytic and PPP metabolites in the cortex (**a**) and spinal cord (**b**)extracts of wild-type and hSOD1^{G93A} mice after injection of [U-^{13}C]glucose at 80 days. Wild-type (black-filled bars, $n = 13$) and hSOD1^{G93A} mice (white-filled bars, $n = 14$) were injected with 0.3 M [U-^{13}C]glucose i.p. The cerebral cortex and spinal cord were dissected and extracted. The total amounts of metabolites were determined by LC-MS/MS. Data represent mean ± SEM and were analyzed using Student's unpaired t test where $p < 0.05$ was set to be significant. G6P, glucose 6-phosphate; F6P, fructose 6-phosphate; F16DP, fructose 1,6-bisphosphate; R5P, ribose 5- phosphate; DHAP, dihydroxyacetone phosphate; (2 + 3) PG, 2 + 3 phosphoglycerate; PEP, phosphoenol pyruvate; PYR, pyruvate

in % ^{13}C enrichments of G6P (M + 6), F16DP (M + 6), and PYR (M + 3) in the cortex, and F6P (M + 6), DHAP (M + 3), 2 + 3 PG (M + 3), and PEP (M + 3) in both the cortex and spinal cord (Table 1).

Total Amounts, % ^{13}C Enrichments, and Cycling Rates of TCA Cycle Intermediates

There were no significant changes between wild-type and hSOD1^{G93A} mice in the total amounts of the TCA cycle metabolites ISO + CIT in the cortex, and ACO, KGA, SUC, FUM, and MAL in both the cortex and spinal cord (Table 2). No significant differences were seen between wild-type and hSOD1^{G93A} mice in the % ^{13}C enrichments of the first-turn TCA cycle metabolites CIT (M + 2) in the cortex, and SUC (M + 2), FUM (M + 2) and SUC (M + 2) in both the cortex and spinal cord (Table 3). Similarly, there were no significant differences in the % ^{13}C enrichments of second turn TCA cycle metabolites CIT (M + 4), SUC (M + 3), and MAL (M + 3), except an increased % ^{13}C enrichment in FUM (M + 3) by 35% in the cortex ($p = 0.033$) of hSOD1^{G93A} mice compared with the wild-type mice (Table 3). Calculating the TCA cycling rates from the ratios of the second turn over the first turn, % enrichments of TCA cycle metabolites showed no differences (Supplementary Table 1).

Total Amounts of Other Energy-Related Metabolites

The total mounts of other energy-related metabolites including glucose 1-phosphate (G1P), guanosine monophosphate (GMP), guanosine diphosphate (GDP), NAD_+, NADH, AMP, ADP, cAMP, glycolate, and the uridine phosphates

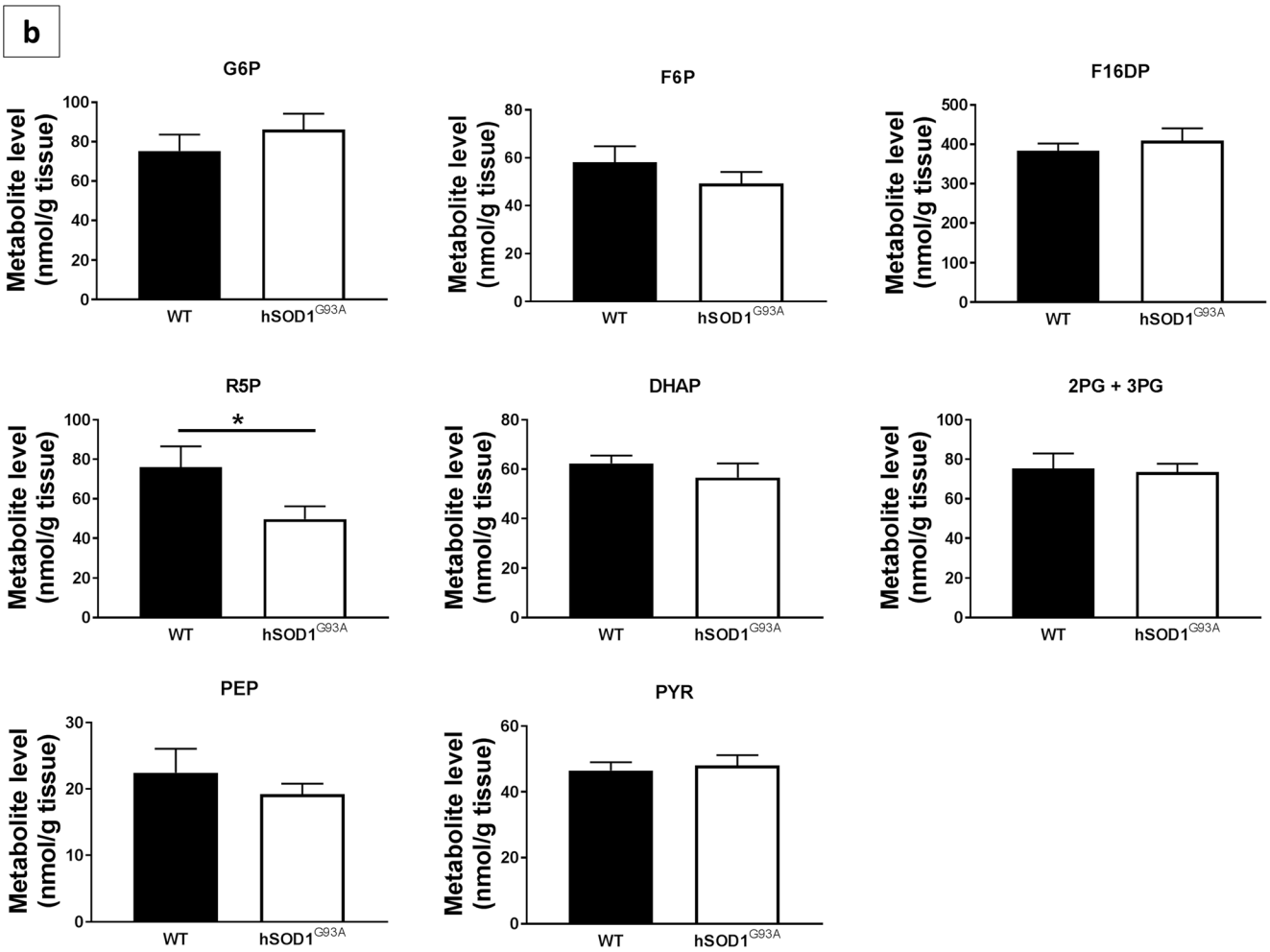

Fig. 2 (continued)

Table 1 The % ^{13}C enrichments of selected glycolytic intermediates in the cortex and spinal cord extracts of wild-type and hSOD1^{G93A} mice after injection of [U-^{13}C]glucose at 80 days

Metabolite	Cortex		Spinal cord	
	WT	hSOD1^{G93A}	WT	hSOD1^{G93A}
G6P (M + 6)	16.75 ± 2.17	19.69 ± 1.32	1.81 ± 0.4	5.68 ± 1.75*
F6P (M + 6)	14.04 ± 2.49	18.5 ± 1.26	ND	ND
F16DP (M + 6)	12.89 ± 1.06	16.2 ± 1.03*	1.22 ± 0.24	1.95 ± 0.44
DHAP (M + 3)	16.1 ± 1.84	18.52 ± 2.04	4.83 ± 0.47	7.00 ± 1.05
(2 + 3)PG (M + 3)	8.02 ± 1.13	8.06 ± 1.21	5.48 ± 0.57	7.18 ± 1.00
PEP (M + 3)	17.42 ± 1.29	18.86 ± 1.76	7.13 ± 1.08	9.38 ± 1.41
PYR (M + 3)	14.83 ± 1.54	17.79 ± 1.35	ND	ND

Wild-type ($n = 11$) and hSOD1^{G93A} mice ($n = 11$) were injected with 0.3 M [U-^{13}C]glucose i.p. The cerebral cortex and spinal cord were dissected and extracted. The total amounts of metabolites were determined by LC-MS/MS. The results were corrected for 1.1% ^{13}C natural abundance. Data represent mean ± SEM and were analyzed using Student's unpaired *t* test where $p < 0.05$ was set to be significant. *G6P*, glucose 6-phosphate; *F6P*, fructose 6-phosphate; *F16DP*, fructose 1,6-bisphosphate; *DHAP*, dihydroxyacetone phosphate; *(2 + 3) PG*, 2 + 3 phosphoglycerate; *PEP*, phosphoenol pyruvate; *PYR*, pyruvate; *ND*, not determined

*Denotes significance

Table 2 Total amounts (nmol/g tissue) of TCA cycle metabolites in the cortex and spinal cord extracts of wild-type and hSOD1^{G93A} mice after injection of [U-^{13}C]glucose at 80 days

Metabolites	Cortex		Spinal cord	
	WT	hSOD1^{G93A}	WT	hSOD1^{G93A}
CIT + ISO	1252 ± 82	1354 ± 36.9	ND	ND
ACO	11.2 ± 1.7	13.0 ± 1.3	2.2 ± 0.2	2.4 ± 0.3
KGA	351.6 ± 59	386.3 ± 42.7	18.1 ± 5.7	28.8 ± 6.3
SUC	112.9 ± 6.4	102.7 ± 9.4	140.3 ± 11.0	141.5 ± 15.1
FUM	311.3 ± 22.1	280.4 ± 7.3	440.7 ± 21.4	440.6 ± 31.9
MAL	362.8 ± 34.8	351.6 ± 40.3	2181 ± 109.7	2266 ± 118.4

Wild-type (black-filled bars, $n = 13$) and hSOD1^{G93A} mice (white-filled bars, $n = 14$) were injected with 0.3 M [U-^{13}C]glucose i.p. The cerebral cortex and spinal cord were dissected and extracted. The total amounts of metabolites were determined by LC-MS/MS. Data represent mean ± SEM and were analyzed using Student's unpaired t test where $p < 0.05$ is set to be significant. *CIT + ISO*, citrate plus isocitrate; *ACO*, aconitate; *KGA*, α-ketoglutarate; *SUC*, succinate; *FUM*, fumarate; *MAL*, malate; *ND*, not determined

(uridine diphosphate (UDP), uridine monophosphate (UMP), uridine diphosphate glucose (UDPG), uridine diphosphate glucoronic acid (UDPGA), and uridine diphosphate *N*-acetyl glucosamine (UDPNAG)) were not significantly altered in the cortex and spinal cord, and guanosine triphosphate (GTP), ATP, NADP, and uridine triphosphate (UTP) in the cortex of wild-type and hSOD1^{G93A} mice at onset of disease (Table 4).

Enzyme Activities

The maximal activities of various enzymes involved in glucose metabolism were investigated in the extracts from the cerebral cortex and spinal cord of wild-type and hSOD1^{G93A} mice at onset of disease (Fig. 3). The activities of the glycolytic enzyme pyruvate kinase and the normalized activities of the TCA cycle enzyme OGDH were significantly reduced in hSOD1^{G93A} mice cortex by 31% ($p = 0.002$, unpaired t test) and 13% ($p = 0.037$, unpaired t test), respectively, compared to wild-type mice (Fig. 3a). Also, there was a 15% reduction in the activities of the PPP enzyme G6PDH in the cortex, although it did not reach statistical significance ($p = 0.058$, unpaired t test) (Fig. 3a). In the spinal cord (Fig. 3b), there was a 24% reduction in G6PDH activity ($p = 0.005$, unpaired t test). Although it did not reach statistical significance ($p = 0.14$, unpaired t test), there was a 22% reduction in OGDH activity in hSOD1^{G93A} mice spinal cord. No significant differences were seen in the activities of HK, PDH, GDH, and GOT in both the cortex (Fig. 3a) and spinal cord (Fig. 3b) and PK in the spinal cord (Fig. 3b) between hSOD1^{G93A} and wild-type mice.

Discussion

The main finding of this study is that the pentose phosphate pathway is impaired, indicated by significant reductions in the concentrations of the PPP metabolite ribose 5-phosphate (R5P), increased % ^{13}C enrichment in G6P, and reduced activity of the PPP enzyme G6PDH in hSOD1^{G93A} mice spinal cord compared to wild-type mice at onset of disease. Also, we showed that the activities of the enzymes pyruvate kinase and the levels of pyruvate in cortex of hSOD1^{G93A} mice were significantly reduced at the onset of disease, which could contribute to impairments in the glycolysis and TCA cycle pathways. OGDH activity was also reduced in the cortex indicating oxidative stress. A summary of the changes in metabolite levels as well as enzyme activities found in the brain and spinal cord tissues of hSOD1^{G93A} mice is given in Fig. 4.

Table 3 The % ^{13}C enrichments of selected 1st and 2nd turn TCA cycle intermediates in the cortex and spinal cord extracts of wild-type and hSOD1^{G93A} mice after injection of [U-^{13}C]glucose at 80 days

Metabolites	Cortex		Spinal cord	
	WT	hSOD1^{G93A}	WT	hSOD1^{G93A}
Citrate M + 2	3.83 ± 0.24	4.26 ± 0.27	1.28 ± 0.11	1.58 ± 0.13
Succinate M + 2	14.38 ± 0.63	15.39 ± 0.54	10.56 ± 0.70	11.5 ± 0.53
Fumarate M + 2	19.38 ± 0.73	20.02 ± 0.72	17.19 ± 0.73	18.03 ± 0.76
Malate M + 2	16.18 ± 0.75	15.58 ± 1.19	13.0 ± 0.63	13.45 ± 0.59
Citrate M + 4	0.38 ± 0.04	0.43 ± 0.03	ND	ND
Succinate M + 3	1.87 ± 0.22	2.19 ± 0.21	2.06 ± 0.24	2.39 ± 0.22
Fumarate M + 3	2.41 ± 0.27	3.26 ± 0.25*	2.81 ± 0.30	3.34 ± 0.29
Malate M + 3	3.01 ± 0.27	3.57 ± 0.30	2.81 ± 0.26	3.11 ± 0.23

Wild-type ($n = 11$) and hSOD1^{G93A} mice ($n = 11$) were injected with 0.3 M [U-^{13}C]glucose i.p. The cerebral cortex and spinal cord were dissected and extracted. The total amounts of metabolites were determined by LC-MS/MS. The results were corrected for 1.1% ^{13}C natural abundance. Data represent mean ± SEM and were analyzed using student's unpaired t test, where $p < 0.05$ was deemed to be significant. *ND*, not determined

*Denotes significance

Table 4 Total amounts (nmol/g tissue) of other energy-related metabolites in cortex (**a**) and spinal cord (**b**) extracts of wild-type and hSOD1^{G93A} mice after injection of [U-^{13}C]glucose at 80 days

Metabolite	Cortex		Spinal cord	
	WT	hSOD1^{G93A}	WT	hSOD1^{G93A}
G1P	20 ± 2.7	25.1 ± 1.9	11.3 ± 1.1	12.8 ± 1.1
GTP	1217 ± 86	1259 ± 97.4	ND	ND
GDP	505 ± 31	580.9 ± 30.7	272.2 ± 27.1	315.2 ± 23.8
GMP	264.5 ± 63.4	164.6 ± 21.1	667.1 ± 31.9	623.5 ± 37.1
Glycolate	72.1 ± 4	77.4 ± 3.8	67 ± 2.6	66 ± 3.6
ATP	3196 ± 512.4	2819 ± 171.5	ND	ND
ADP	3052 ± 269.9	3170 ± 143.3	1245 ± 90.3	1327 ± 73.1
AMP	1153 ± 244.4	905.3 ± 198.1	2689 ± 153.7	2604 ± 194.2
cAMP	3.1 ± 0.3	3.6 ± 0.4	1.1 ± 0.1	1.3 ± 0.1
NAD$^+$	789.5 ± 97.5	975 ± 52.2	33.4 ± 9.6	57.5 ± 18.2
NADH	88.9 ± 12.5	98.8 ± 12.6	43.4 ± 2.9	43.9 ± 1.5
NADP	45.3 ± 4.1	48.6 ± 3.6	ND	ND
UDP	87.4 ± 8.1	87.8 ± 4.7	44.5 ± 4.8	56.6 ± 6.1
UDPG	216.1 ± 13.4	218.8 ± 11.5	173.3 ± 12	185.3 ± 10.7
UDPGA	27.9 ± 1	28.7 ± 1.2	17.8 ± 0.8	16.4 ± 0.7
UDPNAG	209.2 ± 9.8	216.5 ± 10.1	167.8 ± 8.7	161.7 ± 7.9
UMP	102.7 ± 21.8	71.3 ± 13.3	247.8 ± 13.4	236.9 ± 12.3
UTP	452.9 ± 41	493.8 ± 43.7	ND	ND

Wild-type ($n = 13$) and hSOD1^{G93A} mice ($n = 14$) were injected with 0.3 M [U-^{13}C]glucose i.p. Mice were sacrificed 15 min later; the cerebral cortex and spinal cord were dissected out and extracted. The total amounts of metabolites were determined by LC-MS/MS. Data represent mean ± SEM and were analyzed using Student's unpaired *t* test where $p < 0.05$ was deemed to be significant. *ND*, not determined; *G1P*, glucose 1-phosphate; *GMP*, guanosine monophosphate; *GDP*, guanosine diphosphate; *GTP*, guanosine triphosphate; *NAD/NADH*, nicotinamide adenine dinucleotide; *NADP/NADPH*, nicotinamide adenine dinucleotide phosphate; *AMP*, adenosine monophosphate; *ADP*, adenosine triphosphate; *ATP*, adenosine triphosphate; *cAMP*, cyclic adenosine mono phosphate; *UDP*, uridine diphosphate; *UMP*, uridine monophosphate; *UTP*, uridine triphosphate; *UDPG*, uridine diphosphate glucose; *UDPGA*, uridine diphosphate glucoronic acid; *UDPNAG*, uridine diphosphate *N*-acetyl glucosamine

Impaired Pentose Phosphate Pathway in the Spinal Cord of hSOD1^{G93A} Mice

In this study, we found a decrease in the amounts of the PPP metabolite ribose 5-phosphate (R5P) in the spinal cord. We also found an increased % ^{13}C enrichment in G6P in the spinal cord, which most likely signifies reduced metabolism of G6P through the PPP. The PPP and glycolysis are connected via G6P, which is formed by glucose phosphorylation catalyzed by hexokinase. G6P can either enter into glycolysis or the PPP. Via the PPP, G6P generates R5P by the actions of enzymes including G6PDH and 6-phosphogluconate dehydrogenase. The reduction in R5P levels could be due to a reduction in the synthesis of R5P as a result of decreased activities of these enzymes. Consistent with this, we showed that the activity of the main PPP enzyme G6PDH was significantly reduced. Also, studies in NSC-34 models of ALS-transfected with mutant SOD1^{G93A} and SOD1^{G37R} have shown reduced expression and activities of the glucose-6-phosphate dehydrogenase and 6-phosphogluconate dehydrogenase enzymes [26]. The PPP is important to provide pentose sugar molecules for nucleotide synthesis and electrons for generation of NADPH. NADPH is essential to maintain glutathione, a major antioxidant defense molecule in the CNS, in its reduced state. Although the levels of NADPH and glutathione were not measured in this study, the impairment in the PPP is expected to lower their amounts. Overall, decreased PPP increases susceptibility to oxidative stress. Oxidative stress is a key feature of ALS, and several studies have shown increased oxidative damage in proteins, lipids, and DNA in patients with ALS [27–29]. In NSC-34 models of ALS, the reductions in total levels of NADPH [26] and reduced glutathione levels were found, consistent with impairments in the PPP [30]. In addition, depletion of glutathione was found to accelerate cellular death in a NSC-34 cells with TDP43 pathology [31], in the spinal cord of hSOD1^{G93A} mice [32] as well as motor dysfunction and mitochondrial impairments in glutamate-cysteine ligase knockout hSOD1^{G93A} mice [33]. Interestingly, in two studies, glutathione supplementation was able to reduce motor deficits and motor neuron death in the spinal cord [31, 34].

Alterations in Glycolysis in CNS Tissues of hSOD1^{G93A} Mice

We found reduced levels of pyruvate in the cortex of hSOD1^{G93A} mice at the onset of disease indicating reduced glucose metabolism through glycolysis. In agreement with this, we found that the activity of the glycolytic enzyme pyruvate kinase was significantly reduced in the cortex of hSOD1^{G93A} mice. Various studies have shown abnormalities in the glycolytic pathway in CNS tissues of ALS mice. In our previous study, we found diminished levels of glycolytic-derived metabolites, specifically lactate in both the cortex and spinal cord, and alanine in the spinal cord at symptomatic stages of disease [14]. In addition, using FDG-PET and ^{14}C autoradiography, several early studies have shown glucose hypometabolism in the cortex and spinal cord of patients with ALS and animal models of ALS [11–13]. Decreases in glucose uptake together with impairments in glycolysis contribute to a reduction in glycolysis-derived metabolites. Similarly, alterations in enzymes involved in the glycolytic pathway have been reported in ALS. In the motor cortex of patients with ALS, decreased mRNA expression of the glycolytic enzyme 6-phosphofructo-2-kinase (pfkfb3) was found [35]. The enzyme 6-phosphofructo-2-kinase produces fructose 2,6-bisphosphate, which in turn activates the major glycolytic

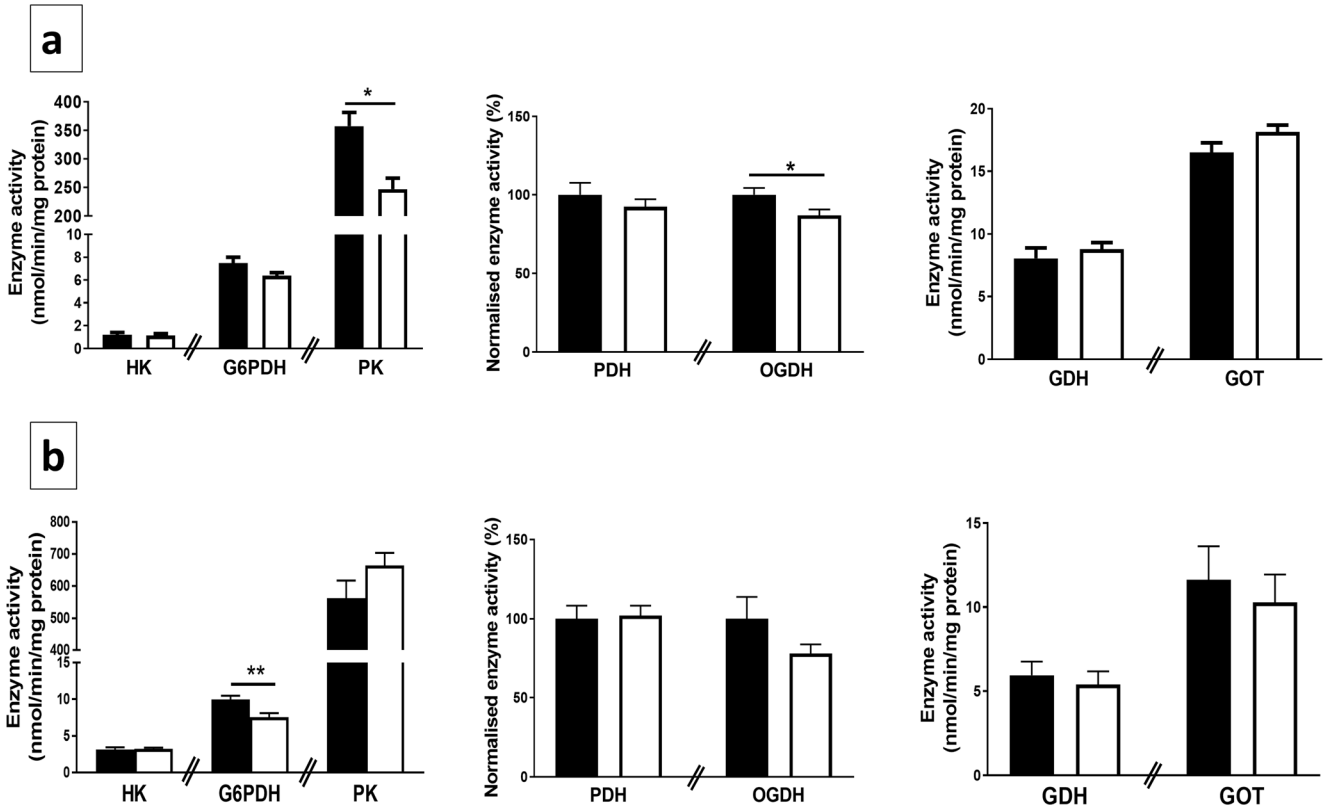

Fig. 3 The maximal activities (U/mg protein) of selected cytosolic enzymes hexokinase (HK), glucose 6-phosphate dehydrogenase (G6PDH), pyruvate kinase (PK), mitochondrial enzymes glutamate dehydrogenase (GDH), glutamic oxaloacetic transaminase (GOT), and normalized enzyme activity (%) of pyruvate dehydrogenase (PDH) and oxoglutarate dehydrogenase (OGDH) in wild-type (WT) and hSOD1^{G93A} mice cortex (**a**) and spinal cord (**b**) at disease onset. PK, GDH, and GOT activities were measured through the oxidation of β-NADH and G6PDH activity via the reduction of β-NADP+ (both at 340 nm) using continuous spectrophotometry. PDH and OGDH activities were measured through the reduction of β-NAD$^+$ at 355 nm emission and 460 nm excitation through continuous fluorometry. Data are represented as mean ± SEM and were analyzed using unpaired Student's *t* test in GraphPad Prism 7 where $*p < 0.05$ and $**p < 0.01$ represent a statistically significant difference between wild-type (black-filled bars) and hSOD1^{G93A} mice (white-filled bars)

enzyme phophofructokinase 1 [36]. Hence, the reduction in the activities of pfkfb3 could lead to slowed glycolysis. Similarly, in astrocytes obtained from hSOD1^{G93A} mice spinal cord, gene expression of the enzyme phosphoglycerate kinase 1 (pgk1) was reduced, also suggesting impairments in glycolysis [19]. The levels of other glycolytic intermediates however were not significantly changed in our study at this early stage of the disease. Generally, the levels of each glycolytic intermediate in the CNS, are low and minor changes may be undetected at this stage of disease [37]. It is important to further investigate the changes in glycolytic metabolism as the disease progresses.

On the other hand, reductions in the levels of pyruvate could arise as a result of an increased shunting of this metabolite into the TCA cycle via pyruvate dehydrogenase (PDH). However, our study did not show increased levels of total or ^{13}C-labeled TCA cycle metabolites. Moreover, studies in hSOD1^{G93A} mutant NSC-34 cells showed increased activities of PDH kinase, an enzyme that reduces PDH enzyme activities [38] suggesting reduced entry of pyruvate into the TCA cycle. Alternatively, pyruvate can be converted to lactate by lactate dehydrogenase. Lactate can then be transferred into the blood and contribute to the reduction in the amounts of pyruvate. Increased blood lactate levels have been found in patients with ALS [39, 40]. Increased glycogen formation may also contribute to low lactate levels. Glycogen levels were found to be high in hSOD1^{G93A} mice brainstem and lumbar spinal cord [41]. Taken together, impairments in glucose metabolism via glycolysis could contribute to diminished production of ATP in CNS tissues in ALS.

TCA Cycle Intermediate Levels Were Largely Unchanged

The incorporation of ^{13}C in TCA cycle intermediates was mainly unchanged at the onset stage of disease except for an increase in % ^{13}C enrichment in fumarate in the cortex in the second turn of the TCA cycle, which may be caused by the trend towards the reduction in the total amounts of fumarate. Although the total amounts of TCA cycle intermediates were largely unchanged, we found reduced activity of the TCA cycle enzyme OGDH in the cortex at the onset of

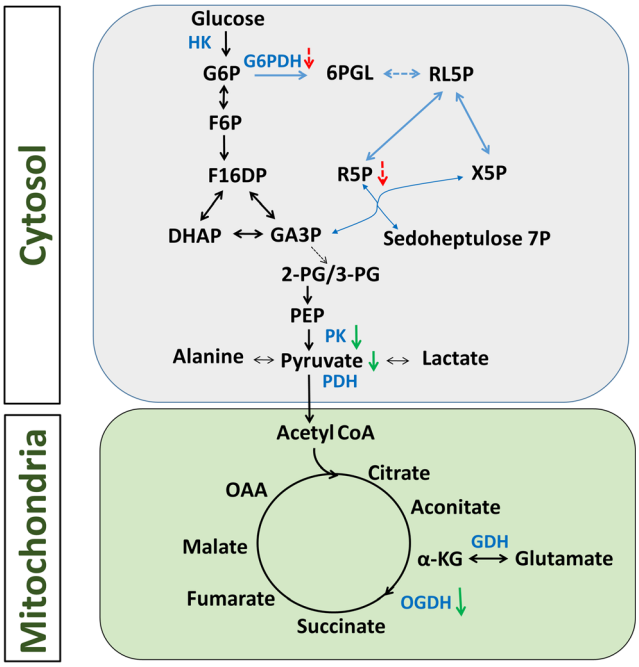

Fig. 4 Summary of alterations in the levels of metabolites and enzyme activities in the brain and spinal cord of ALS mice. Changes in the spinal cord are shown in red-dotted arrows, while the green arrows show changes in the cortex. The levels of glucose, 6PGL, RL5P, X5P, sedoheptulose 7P, acetyl-CoA, lactate, and glutamate were not measured. G6P, glucose 6-phosphate; 6PGL, 6-phospho gluconolactone; F6P, fructose 6-phosphate; F16DP, fructose 1,6-bisphosphate; DHAP, dihydroxyacetone phosphate; GA3P, glyceraldehyde 3-phosphate; (2/3) PG, 2 + 3 phosphoglycerate; PEP, phosphoenol pyruvate; RL5P, ribulose 5-phosphate; R5P, ribose 5-phosphate; X5P, xylulose 5-phosphate; OAA, oxaloacetate; α-KG, α-ketoglutarate; HK, hexokinase; G6PDH, glucose 6-phosphate dehydrogenase; PK, pyruvate kinase; PDH, pyruvate dehydrogenase; GDH, glutamate dehydrogenase; OGDH, oxoglutarate dehydrogenase

disease, which may indicate elevated oxidative stress. Increased oxidative stress has been shown to inhibit OGDH and other TCA cycle enzymes in isolated nerve terminals and various cellular systems [42, 43]. In our previous study, some of the first-turn TCA cycle–derived neurotransmitters were reduced in the spinal cord at mid stage (120 days), which could be due to the reduced entry of pyruvate into the TCA cycle [14]. Other studies have shown abnormalities in the enzymes involved in the TCA cycle, such as reduced gene expression of isocitrate dehydrogenase and oxoglutarate dehydrogenase in hSOD1^{G93A} mice spinal cord [18, 19], and increased expression of PDH kinase 1, an enzyme which inactivates PDH in NSC-34 cells from SOD1^{G93A} mice [38]. Conversely, substances that feed the TCA cycle were shown to delay loss of motor neurons and improve motor symptoms in hSOD1^{G93A} mouse model of ALS [44, 45]. In this study, the TCA cycle appears to generally function normally at the onset of disease. In future experiments, changes in these energy-producing pathways need to be further characterized as the disease progresses.

Alternative Fuels and Antioxidants Could Correct Metabolic Abnormalities in ALS

Given the impairments found in the CNS glucose metabolism, particularly in glycolysis and the PPP, alternative fuels may aid in providing energy to neurons and delay disease progression in ALS [20]. Studies using substances that provide additional energy such as caprylic triglyceride [49], ketogenic diet [50], triheptanoin [44], and the "Deanna Protocol," a combination of metabolic supplements including medium chain triglycerides and arginine α-ketoglutarate [45], were shown to improve motor symptoms and protect loss of motor neurons in ALS animal models. Moreover, the impairments observed in the PPP could lead to reduced ability of the CNS to defend against oxidative stress. In light of increased oxidative stress found in ALS, several antioxidant molecules have been investigated and were shown to protect against motor neuron degeneration in models of ALS (Matthews et al. 1998; Cassina et al. 2008; Miquel et al. 2014). Clinical trials testing alternative fuels and antioxidants are limited, and there is a need to further assess the therapeutic effects of such substances in people with ALS. Recently, edaravone, an antioxidant molecule was approved by the FDA for the treatment of ALS, which further raises the hope of better treatment [51].

Conclusion

In conclusion, we demonstrated impairments in the pentose phosphate and glycolytic pathways in hSOD1^{G93A} mice CNS tissues at the onset of disease, which are expected to lead increased oxidative stress. Also, this will impair ATP generation and contribute to subsequent energy deficit in ALS. These findings emphasize the role of metabolic dysfunction in the pathogenesis and progression of ALS and the need to correct metabolic abnormalities and protection against oxidative stress to improve outcomes.

Acknowledgements We wish to thank the Queensland Brain Institute and Dr. Shuyan Ngo for providing animals. TWT is a recipient of The University of Queensland International scholarship.

Funding This work was supported by the Motor Neurone Disease Research Institute Australia to KB (grant number: GIA 1704).

Compliance with Ethical Standards All animal experiments were approved by the University of Queensland Animal Ethics Committee (SBMS 128/14) and followed the guidelines of the Queensland Animal Care and Protection Act 2001.

Conflict of Interest The authors declare that they have no conflicts of interest.

References

1. Kiernan MC, Vucic S, Cheah BC, Turner MR, Eisen A, Hardiman O, Burrell JR, Zoing MC (2011) Amyotrophic lateral sclerosis. Lancet 377(9769):942–955. https://doi.org/10.1016/S0140-6736(10)61156-7
2. Chen S, Sayana P, Zhang X, Le W (2013) Genetics of amyotrophic lateral sclerosis: an update. Mol Neurodegener 8:28. https://doi.org/10.1186/1750-1326-8-28
3. Sreedharan J, Blair IP, Tripathi VB, Hu X, Vance C, Rogelj B, Ackerley S, Durnall JC et al (2008) TDP-43 mutations in familial and sporadic amyotrophic lateral sclerosis. Science 319(5870):1668–1672. https://doi.org/10.1126/science.1154584
4. Rothstein JD, Martin LJ, Kuncl RW (1992) Decreased glutamate transport by the brain and spinal cord in amyotrophic lateral sclerosis. N Engl J Med 326(22):1464–1468. https://doi.org/10.1056/NEJM199205283262204
5. Rothstein JD (1995) Excitotoxic mechanisms in the pathogenesis of amyotrophic lateral sclerosis. Adv Neurol 68:7–20 discussion 21-27
6. Shaw PJ, Ince PG, Falkous G, Mantle D (1995) Oxidative damage to protein in sporadic motor neuron disease spinal cord. Ann Neurol 38(4):691–695. https://doi.org/10.1002/ana.410380424
7. Dupuis L, Oudart H, Rene F, Gonzalez de Aguilar JL, Loeffler JP (2004) Evidence for defective energy homeostasis in amyotrophic lateral sclerosis: benefit of a high-energy diet in a transgenic mouse model. Proc Natl Acad Sci U S A 101(30):11159–11164. https://doi.org/10.1073/pnas.0402026101
8. Dupuis L, Pradat PF, Ludolph AC, Loeffler JP (2011) Energy metabolism in amyotrophic lateral sclerosis. Lancet Neurol 10(1):75–82. https://doi.org/10.1016/S1474-4422(10)70224-6
9. Korner S, Hendricks M, Kollewe K, Zapf A, Dengler R, Silani V, Petri S (2013) Weight loss, dysphagia and supplement intake in patients with amyotrophic lateral sclerosis (ALS): impact on quality of life and therapeutic options. BMC Neurol 13:84. https://doi.org/10.1186/1471-2377-13-84
10. Desport JC, Preux PM, Magy L, Boirie Y, Vallat JM, Beaufrere B, Couratier P (2001) Factors correlated with hypermetabolism in patients with amyotrophic lateral sclerosis. Am J Clin Nutr 74(3):328–334
11. Browne SE, Yang L, DiMauro JP, Fuller SW, Licata SC, Beal MF (2006) Bioenergetic abnormalities in discrete cerebral motor pathways presage spinal cord pathology in the G93A SOD1 mouse model of ALS. Neurobiol Dis 22(3):599–610. https://doi.org/10.1016/j.nbd.2006.01.001
12. Miyazaki K, Masamoto K, Morimoto N, Kurata T, Mimoto T, Obata T, Kanno I, Abe K (2012) Early and progressive impairment of spinal blood flow-glucose metabolism coupling in motor neuron degeneration of ALS model mice. J Cereb Blood Flow Metab 32(3):456–467. https://doi.org/10.1038/jcbfm.2011.155
13. Dalakas MC, Hatazawa J, Brooks RA, Di Chiro G (1987) Lowered cerebral glucose utilization in amyotrophic lateral sclerosis. Ann Neurol 22(5):580–586. https://doi.org/10.1002/ana.410220504
14. Tefera TW, Borges K (2018) Neuronal glucose metabolism is impaired while astrocytic TCA cycling is unaffected at symptomatic stages in the hSOD1(G93A) mouse model of amyotrophic lateral sclerosis. J Cereb Blood Flow Metab:271678X18764775. https://doi.org/10.1177/0271678X18764775
15. Barber SC, Mead RJ, Shaw PJ (2006) Oxidative stress in ALS: a mechanism of neurodegeneration and a therapeutic target. Biochim Biophys Acta 1762(11–12):1051–1067. https://doi.org/10.1016/j.bbadis.2006.03.008
16. Niedzielska E, Smaga I, Gawlik M, Moniczewski A, Stankowicz P, Pera J, Filip M (2016) Oxidative stress in neurodegenerative diseases. Mol Neurobiol 53(6):4094–4125. https://doi.org/10.1007/s12035-015-9337-5
17. Veyrat-Durebex C, Corcia P, Piver E, Devos D, Dangoumau A, Gouel F, Vourc'h P, Emond P et al (2015) Disruption of TCA cycle and glutamate metabolism identified by metabolomics in an in vitro model of amyotrophic lateral sclerosis. Mol Neurobiol 53:6910–6924. https://doi.org/10.1007/s12035-015-9567-6
18. D'Arrigo A, Colavito D, Pena-Altamira E, Fabris M, Dam M, Contestabile A, Leon A (2010) Transcriptional profiling in the lumbar spinal cord of a mouse model of amyotrophic lateral sclerosis: a role for wild-type superoxide dismutase 1 in sporadic disease? J Mol Neurosci 41(3):404–415. https://doi.org/10.1007/s12031-010-9332-2
19. Ferraiuolo L, Higginbottom A, Heath PR, Barber S, Greenald D, Kirby J, Shaw PJ (2011) Dysregulation of astrocyte-motoneuron cross-talk in mutant superoxide dismutase 1-related amyotrophic lateral sclerosis. Brain 134(Pt 9):2627–2641. https://doi.org/10.1093/brain/awr193
20. Tefera TW, Borges K (2016) Metabolic dysfunctions in amyotrophic lateral sclerosis pathogenesis and potential metabolic treatments. Front Neurosci 10:611. https://doi.org/10.3389/fnins.2016.00611
21. Tefera TW, Tan KN, McDonald TS, Borges K (2016) Alternative fuels in epilepsy and amyotrophic lateral sclerosis. Neurochem Res 42:1610–1620. https://doi.org/10.1007/s11064-016-2106-7
22. Le Belle JE, Harris NG, Williams SR, Bhakoo KK (2002) A comparison of cell and tissue extraction techniques using high-resolution 1H-NMR spectroscopy. NMR Biomed 15(1):37–44
23. McDonald TS, Carrasco-Pozo C, Hodson MP, Borges K (2017) Alterations in cytosolic and mitochondrial [U-13C]glucose metabolism in a chronic epilepsy mouse model. eNeuro 4(1):ENEURO.0341–ENEU16.2017. https://doi.org/10.1523/ENEURO.0341-16.2017
24. Medina-Torres CE, van Eps AW, Nielsen LK, Hodson MP (2015) A liquid chromatography-tandem mass spectrometry-based investigation of the lamellar interstitial metabolome in healthy horses and during experimental laminitis induction. Vet J 206(2):161–169. https://doi.org/10.1016/j.tvjl.2015.07.031
25. Tan KN, Simmons D, Carrasco-Pozo C, Borges K (2018) Triheptanoin protects against status epilepticus-induced hippocampal mitochondrial dysfunctions, oxidative stress and neuronal degeneration. J Neurochem 144(4):431–442. https://doi.org/10.1111/jnc.14275
26. Kirby J, Halligan E, Baptista MJ, Allen S, Heath PR, Holden H, Barber SC, Loynes CA et al (2005) Mutant SOD1 alters the motor neuronal transcriptome: implications for familial ALS. Brain 128(Pt 7):1686–1706. https://doi.org/10.1093/brain/awh503
27. Bowling AC, Schulz JB, Brown RH Jr, Beal MF (1993) Superoxide dismutase activity, oxidative damage, and mitochondrial energy metabolism in familial and sporadic amyotrophic lateral sclerosis. J Neurochem 61(6):2322–2325
28. Mitsumoto H, Santella RM, Liu X, Bogdanov M, Zipprich J, Wu HC, Mahata J, Kilty M et al (2008) Oxidative stress biomarkers in sporadic ALS. Amyotroph Lateral Scler 9(3):177–183. https://doi.org/10.1080/17482960801933942
29. Simpson EP, Henry YK, Henkel JS, Smith RG, Appel SH (2004) Increased lipid peroxidation in sera of ALS patients: a potential biomarker of disease burden. Neurology 62(10):1758–1765
30. Allen S, Heath PR, Kirby J, Wharton SB, Cookson MR, Menzies FM, Banks RE, Shaw PJ (2003) Analysis of the cytosolic proteome in a cell culture model of familial amyotrophic lateral sclerosis reveals alterations to the proteasome, antioxidant defenses, and nitric oxide synthetic pathways. J Biol Chem 278(8):6371–6383. https://doi.org/10.1074/jbc.M209915200
31. Chen T, Turner BJ, Beart PM, Sheehan-Hennessy L, Elekwachi C, Muyderman H (2017) Glutathione monoethyl ester prevents TDP-43 pathology in motor neuronal NSC-34 cells. Neurochem Int 112:278–287. https://doi.org/10.1016/j.neuint.2017.08.009

32. Chi L, Ke Y, Luo C, Gozal D, Liu R (2007) Depletion of reduced glutathione enhances motor neuron degeneration in vitro and in vivo. Neuroscience 144(3):991–1003. https://doi.org/10.1016/j.neuroscience.2006.09.064
33. Vargas MR, Johnson DA, Johnson JA (2011) Decreased glutathione accelerates neurological deficit and mitochondrial pathology in familial ALS-linked hSOD1(G93A) mice model. Neurobiol Dis 43(3):543–551. https://doi.org/10.1016/j.nbd.2011.04.025
34. Santa-Cruz LD, Tapia R (2014) Role of energy metabolic deficits and oxidative stress in excitotoxic spinal motor neuron degeneration in vivo. ASN Neuro 6(2):AN20130046. https://doi.org/10.1042/AN20130046
35. Wang XS, Simmons Z, Liu W, Boyer PJ, Connor JR (2006) Differential expression of genes in amyotrophic lateral sclerosis revealed by profiling the post mortem cortex. Amyotroph Lateral Scler 7(4):201–210. https://doi.org/10.1080/17482960600947689
36. Herrero-Mendez A, Almeida A, Fernandez E, Maestre C, Moncada S, Bolanos JP (2009) The bioenergetic and antioxidant status of neurons is controlled by continuous degradation of a key glycolytic enzyme by APC/C-Cdh1. Nat Cell Biol 11(6):747–752. https://doi.org/10.1038/ncb1881
37. Dienel GA (2014) Chapter 3 - energy metabolism in the brain. In: From molecules to networks, 3rd edn. Academic, Boston, pp. 53–117. https://doi.org/10.1016/B978-0-12-397179-1.00003-8
38. D'Alessandro G, Calcagno E, Tartari S, Rizzardini M, Invernizzi RW, Cantoni L (2011) Glutamate and glutathione interplay in a motor neuronal model of amyotrophic lateral sclerosis reveals altered energy metabolism. Neurobiol Dis 43(2):346–355. https://doi.org/10.1016/j.nbd.2011.04.003
39. Siciliano G, Pastorini E, Pasquali L, Manca ML, Iudice A, Murri L (2001) Impaired oxidative metabolism in exercising muscle from ALS patients. J Neurol Sci 191(1–2):61–65
40. Siciliano G, D'Avino C, Del Corona A, Barsacchi R, Kusmic C, Rocchi A, Pastorini E, Murri L (2002) Impaired oxidative metabolism and lipid peroxidation in exercising muscle from ALS patients. Amyotroph Lateral Scler Other Motor Neuron Disord 3(2):57–62. https://doi.org/10.1080/146608202760196011
41. Dodge JC, Treleaven CM, Fidler JA, Tamsett TJ, Bao C, Searles M, Taksir TV, Misra K et al (2013) Metabolic signatures of amyotrophic lateral sclerosis reveal insights into disease pathogenesis. Proc Natl Acad Sci U S A 110(26):10812–10817. https://doi.org/10.1073/pnas.1308421110
42. Tretter L, Adam-Vizi V (2000) Inhibition of Krebs cycle enzymes by hydrogen peroxide: a key role of [alpha]-ketoglutarate dehydrogenase in limiting NADH production under oxidative stress. J Neurosci 20(24):8972–8979
43. Mailloux RJ, Beriault R, Lemire J, Singh R, Chenier DR, Hamel RD, Appanna VD (2007) The tricarboxylic acid cycle, an ancient metabolic network with a novel twist. PLoS One 2(8):e690. https://doi.org/10.1371/journal.pone.0000690
44. Tefera TW, Wong Y, Barkl-Luke ME, Ngo ST, Thomas NK, McDonald TS, Borges K (2016) Triheptanoin protects motor neurons and delays the onset of motor symptoms in a mouse model of amyotrophic lateral sclerosis. PLoS One 11(8):e0161816. https://doi.org/10.1371/journal.pone.0161816
45. Ari C, Poff AM, Held HE, Landon CS, Goldhagen CR, Mavromates N, D'Agostino DP (2014) Metabolic therapy with Deanna protocol supplementation delays disease progression and extends survival in amyotrophic lateral sclerosis (ALS) mouse model. PLoS One 9(7):e103526. https://doi.org/10.1371/journal.pone.0103526
46. Matthews RT, Yang L, Browne S, Baik M, Beal MF (1998) Coenzyme Q10 administration increases brain mitochondrial concentrations and exerts neuroprotective effects. Proc Natl Acad Sci U S A 95 (15):8892–8897
47. Cassina P, Cassina A, Pehar M, Castellanos R, Gandelman M, de Leon A, Robinson KM, Mason RP, Beckman JS, Barbeito L, Radi R (2008) Mitochondrial dysfunction in SOD1G93A-bearing astrocytes promotes motor neuron degeneration: prevention by mitochondrial-targeted antioxidants. J Neurosci 28(16):4115–4122. https://doi.org/10.1523/JNEUROSCI.5308-07.2008
48. Miquel E, Cassina A, Martinez-Palma L, Souza JM, Bolatto C, Rodriguez-Bottero S, Logan A, Smith RA, Murphy MP, Barbeito L, Radi R, Cassina P (2014) Neuroprotective effects of the mitochondria-targeted antioxidant MitoQ in a model of inherited amyotrophic lateral sclerosis. Free Radic Biol Med 70:204–213. https://doi.org/10.1016/j.freeradbiomed.2014.02.019
49. Zhao W, Varghese M, Vempati P, Dzhun A, Cheng A, Wang J, Lange D, Bilski A et al (2012) Caprylic triglyceride as a novel therapeutic approach to effectively improve the performance and attenuate the symptoms due to the motor neuron loss in ALS disease. PLoS One 7(11):e49191. https://doi.org/10.1371/journal.pone.0049191
50. Zhao Z, Lange DJ, Voustianiouk A, MacGrogan D, Ho L, Suh J, Humala N, Thiyagarajan M et al (2006) A ketogenic diet as a potential novel therapeutic intervention in amyotrophic lateral sclerosis. BMC Neurosci 7(29):29. https://doi.org/10.1186/1471-2202-7-29
51. Scott A (2017) Drug therapy: on the treatment trail for ALS. Nature 550(7676):S120–S121. https://doi.org/10.1038/550S120a